APPLICABILITY OF THE INDENTATION-STRENGTH METHOD TO THE MEASUREMENT OF THE CRACK RESISTANCE CURVE IN BRITTLE MATERIALS

L. Bertamini, R. Dal Maschio, T. Riccò*

A suitable and accurate characterization of the R-curve effect in ceramics would be extremely useful in their practical applications. The aim of the present work is to check the accuracy of the indentation-strength-by- bending (ISB) methodology for measuring the crack resistance curve, taking polymethylmethacrylate (PMMA) as a reference material.

INTRODUCTION

Recent studies have shown that the resistance of many polycrystalline ceramics to crack propagation increases with crack length (R-curve effect), which is due to cumulative crack/microstructure interactions in the polycrystal. Since this effect has significant practical consequences, such as flaw tolerance and promotion of crack stability, it needs to be properly characterized, given the engineering applications of these materials. The poor machinability of ceramics makes it difficult to use conventional fracture mechanics techniques for toughness measurements, particularly in routine evaluations.

* Department of Materials Engineering, University of Trento

To overcome this problem, fracture indentation techniques have been developed. However, the data mentioned in literature, obtained by that method, show, for a same material, a high dispersion, that could be attributed either to the inaccuracy inherent in the method or to the non-reproducibility of the material's microstructure. The present work treats the former aspect, and is aimed at evaluating the accuracy of the indentation-strength methodology for measuring the crack resistance curve. To this end, polymethylmethacrylate (PMMA) was chosen as a reference material due to its particular characteristics, such as good machinability, high homogeneity and trasparency. For this material the R-curve was measured by two different methods i) the indentation-strength- by-bending (ISB) technique and ii) a single-specimen technique based on video-recording of the crack growth during the test.

EXPERIMENTAL PROCEDURE

ISB tests were performed on PMMA bars machined from a cast sheet, supplied by VEDRIL S.p.A., Milano (I), to dimensions of 120 x 8 x 6 mm . The sawing surfaces were then polished with SiC grinding paper and subsequently with 6 μm diamond paste. Controlled surface flaws were introduced by a Vickers diamond pyramid indenter with indentation loads ranging from 3 to 10 N and a contact time of 30 sec. All indentations were made at room temperature through a drop of acetone, placed on the contact surface during the indent period to provide an aggressive environment that enhanced crack formation. Care was taken to align radial cracks perpendicular and parallel to the longitudinal axis of the specimen. After indentation, the samples were tested in four-point bending with an outer span of 80 mm and an inner span of 40 mm, and with the surface containing the indentation flaw on the tension side. The tests were conducted in air at room temperature at a crosshead speed of 1 mm/min.

SE(B) specimens , measuring 55 x 12.5 x 6 mm, with the sawing surfaces treated by the same procedure as above,were razor-blade sharply notched on one side to a notch-to-width ratio a_0/W of about 0.5. SE(B) tests with a span of 50 mm were carried out at room temperature at a crosshead speed of 1 mm/min. Real-time visualization and recording of the crack growth was obtained with a videocamera. The shooting and load-recording were synchronized for subsequent quantitative evaluation.

RESULTS AND DISCUSSION

When a sufficient load P is applied to a sharp indenter in contact with a test material and the indenter is then unloaded, the surface length 2c of the semicircular radial cracks that develop in the material is related to P, according to the indentation fracture mechanics model (1,2), valid for ceramics and inorganic glasses, as follows

$$c = \left[\chi_r \frac{P}{K_{IC}}\right]^{\frac{2}{3}} \tag{1}$$

in which K_{Ic} is the critical stress intensity factor and χ_r is a constant. For PMMA, the experimental values of c and P have been found to fit an equation similar to eq.1, but with a lower power (3). It has been shown that this result is connected to a R-curve effect, which implies that the toughness, K_{Ic}, increases with crack length. Moreover, for PMMA, it has been found, as shown in Fig. 1, that the configuration of the indentation cracks is not semicircular, but rather of the Palmqvist type. The particular shape of these cracks suggests that the crack depth d_o (see Fig. 1) should be the essential flaw dimension that governs the strength of PMMA in the subsequent bending tests . During a strength test on an indented specimen, the residual force that still persists after indentation supplements the applied tension in driving the radial crack to failure . Thus, the applied net stress intensity factor K is the sum of that due to the residual force and that due to the applied stress (4):

$$K = \frac{P\,\chi_r}{d^{3/2}} + \Omega\,\sigma_a\,d^{1/2} \tag{2}$$

in which σ_a is the applied stress,d is the Palmqvist crack depth and Ω is a shape factor equal to 1.01 (4).

To facilitate analysis of indentation strength data for materials that display R-curve effect, a fractional power law is generally used to represent the crack resistance curve :

$$K_R = k\, d^{\,m} \tag{3}$$

in which k and m are constants (4). The exponent m measures the susceptibility to R-curve behaviour: when m is zero, K_R is invariant with crack extension. An applied stress-equilibrium crack size function follows from eq. 2 by taking $K = K_{Ic}$, assuming from eq. 3 that $K_R = K_{Ic} = kd^m$ and solving for σ_a

$$\sigma_a = \frac{1}{\Omega\, d^{\,1/2}}\left[k\, d^{\,m} - \frac{\chi_r P}{d^{3/2}}\right] \tag{4}$$

For $\chi_r>0$ and $m<0.5$, eq. 4 exhibits a maximum for

$$d_m = \left[\frac{4\,\chi_r P}{k(1-2m)}\right]^{\frac{2}{2m+3}} \tag{5}$$

$$\sigma_m = \frac{k}{\Omega}\left[\frac{2m+3}{4}\right]\left[\frac{4\,\chi_r P}{k(1-2m)}\right]^{\frac{2m-1}{2m+3}} \tag{6}$$

The crack extends stably from d_o to d_m before failure occurs at $\sigma_a = \sigma_m$.

By introducing eq. 5 into eq. 6, a direct correlation between d_m and σ_m is obtained :

$$\sigma_m = \frac{k}{\Omega}\left[\frac{2m+3}{4}\right] d_m^{\frac{2m-1}{2}} \tag{7}$$

This relationship has been used to obtain m and k from the experimental data (m = 0.26 and k = 11.6), in substantial agreement with Ritter et al. (3). The value obtained for m together with the experimental data for σ_m and d_m were used to evaluate the R-curve by means of eq. 3 and eq. 7 (Fig. 2).

In SE(B) tests, the video-recording of the fracture process revealed that the crack starts from the initial straight notch at specimen mid-thickness, growing stably with a bowed front shape through the entire thickness of the specimen till it becomes unstable. The results for K_R during the stable growth of the crack are given in Fig. 3 as a function of the variation of the crack depth Δa. The values of K_R obtained with the two different methods are given as a function of the crack surface area A in Fig. 4. It appears that the two sets of data, though covering partially different ranges of A, fairly closely fit the same R-curve.

CONCLUDING REMARKS

Comparison of the results obtained with the two different methods indicates the "intrinsic" accuracy of the ISB methodology for evaluating the crack resistance curve. This method can, therefore, be considered particularly attractive and promising for characterizing the R-curve effect in ceramic materials, also in consideration of its experimental simplicity with respect to other fracture mechanics techniques.

REFERENCES

(1) Anstis, G. R., Chantikul, P., Lawn, B. R., and Marshall, D.B., Am. Ceram. Soc., Vol. 64, 1981, p. 533.

(2) Lawn, B. R., Evans, A. G., and Marshall, D. B., J. Am. Ceram. Soc., Vol. 63, 1980, p. 574.

(3) Ritter, J. E., Lin, M.R., and Lardner, T. J., J. Mater. Sci., Vol. 23, 1988, pp. 2370 - 2378.

(4) Krause, R. F., J. Am. Ceram. Soc., Vol. 71, 1988, pp. 338 - 343.

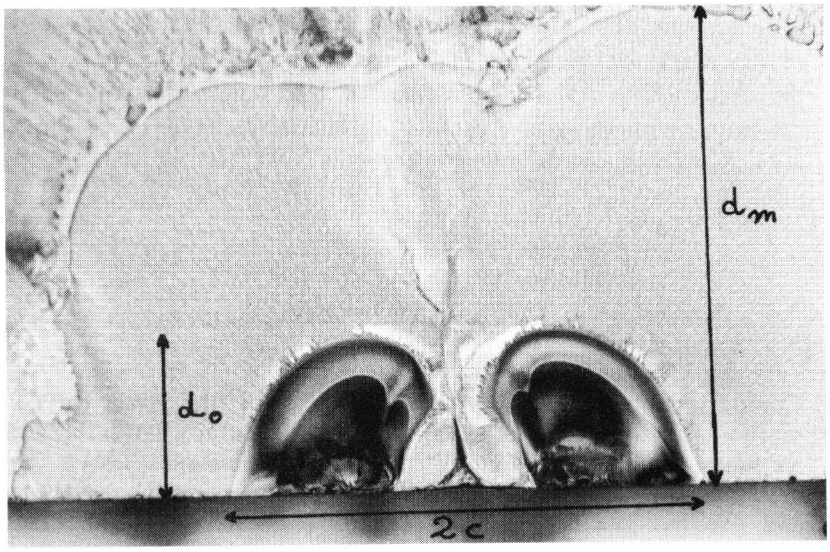

Figure 1 Fracture surface of a PMMA sample after ISB testing.

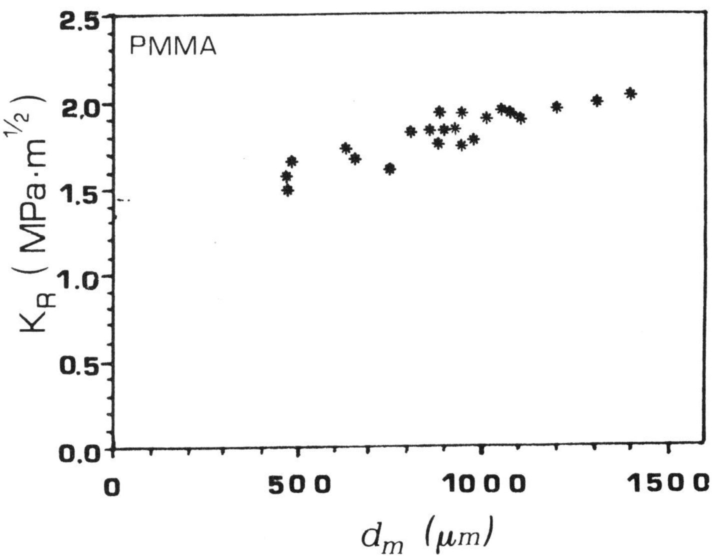

Figure 2 R-curve obtained by ISB methodology.

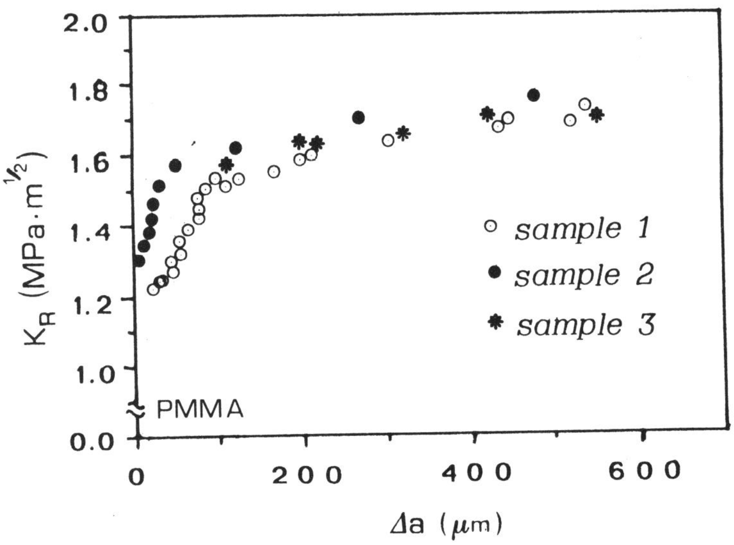

Figure 3 R- curve obtained by SE(B) tests (see text).

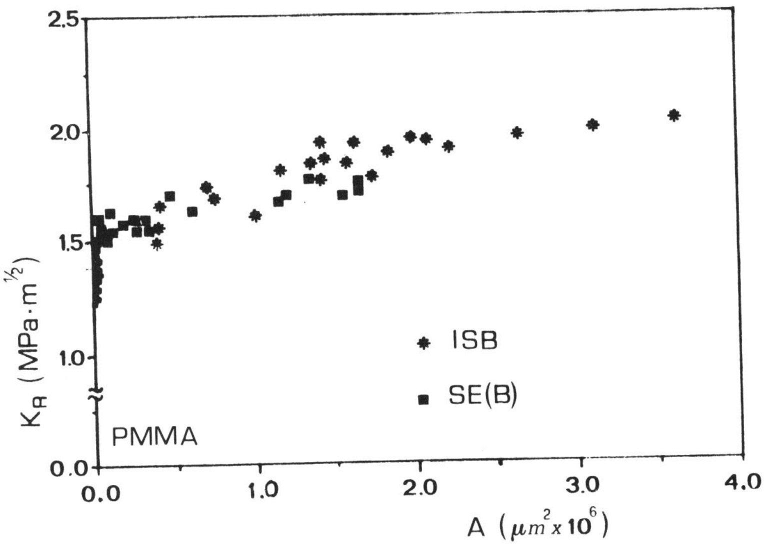

Figure 4 Comparison of the R-curves obtained by the two different techniques considered .